

Modeling on ^{137}Cs Radioactive Dispersion in Gosong Coast as The Candidate Location for Nuclear Power Plant

Akhmad Tri Prasetyo¹, Muslim^{2*}, Heny Suseno³

¹Department of Marine Sciences, Faculty of Fisheries and Marine Sciences, Diponegoro University

²Department of Oceanography, Faculty of Fisheries and Marine Sciences, Diponegoro University
Jl. Prof. Sudarto, Tembalang, Semarang, Central Java 50275 Indonesia

³Center for Radiation Safety and Metrology – National Nuclear Energy Agency
Lebak Bulus Raya Street, Number 49 Lebak Bulus, Cilandak, Jakarta 12440

Email: aqua_muslim@yahoo.com

Abstract

The study of radioactive dispersion in the ocean should be conducted to prepare the construction of nuclear power plant (NPP) in Gosong Coast, West Kalimantan. This study estimated the distribution of ^{137}Cs radioactive from various scenarios of radioactive waste dumping if nuclear emergency is occurred during NPP's operation. These scenarios were distinguished based on their volume discharges of radioactive waste into the ocean, included 10 m³ (Scenario I), 50 m³ (Scenario II), and 100 m³ (Scenario III). Model dispersions were constructed for 15 days by Delft3D-Flow module. The simulation showed that ocean current directions were not significantly different among spring and neap tide, instead the ocean current during the spring period dominantly increased rather than neap period. Ocean currents at Gosong Coast flowed parallel to the shoreline towards Singkawang Coastal Area during ebb tide. Meanwhile, during flood tide, ocean currents at Gosong Coast flowed offshore through Burung Archipelagic. The dispersed model showed the distribution of ^{137}Cs radioactive for 15 days reaching to coastal areas of Burung Archipelagic, Singkawang, and Southern Sambas Coast. Each scenario of the disposal system did not influence the marine pollution of the West Kalimantan Sea.

Keywords : Gosong Coast, Nuclear Power Plant, ^{137}Cs Dispersion, Hydrodynamical Model

INTRODUCTION

The Indonesian government planned to build the nuclear reactor as the electrical source in Gosong Coast, West Kalimantan (Provincial government of West Kalimantan, 2019). This policy followed Presidential Decree Number 6 in 2006 about the national energy policy in Indonesia, nuclear power plant (NPP) will contribute about 2% of Indonesia's total electricity in 2025. The operation of NPP should not discharge its radioactive waste into the environment, instead it will be stored in the underground disposal facility (Muslim *et al.*, 2016). Firstly, radioactive waste should be processed before it will be saved in disposal facility, such as chemical reprocessing, decontamination, decommissioning, and other fuel cycles. These processes divide

radioactive waste into two levels which are high-level waste (HLW) and low-intermediate level waste (LILW). HLW will be stored in the deep underground facility, while LILW will be stored in the near-surface facility (IAEA, 2009). However, it is still possible to release radioactive wastes with low level into the sea in nuclear emergency, such as the planned release of radioactive waste at the Fukushima NPP (Periáñez *et al.*, 2021). Furthermore, radioactive wastes potentially pollute the marine environment (Fulghum *et al.*, 2019).

Anthropogenic radionuclides are created from the process of nuclear fission reactions through the application of nuclear technology by humans, such as nuclear weapons or nuclear electrical energy (Alkatiri *et al.*, 2019; Aoyama *et al.*, 2020). The ^{137}Cs

*) Corresponding author
www.ejournal2.undip.ac.id/index.php/jkt

substrate is one of anthropogenic radionuclides which is contained in NPP waste (Kawamura *et al.*, 2017; Muslim *et al.*, 2016) and has 30 years half-life (Sakuma *et al.*, 2019; Tsumune *et al.*, 2020). This radionuclide is the conservative radionuclide that remains dissolved in the water column instead of adsorption in bed sediment (Periáñez *et al.*, 2019). Its presence in the ocean can lead the radiation doses to marine organisms (Fulghum *et al.*, 2019). Furthermore, humans will be affected as well when they are consuming seafood from this ocean.

Many studies on the dispersion model of radioactive waste in the ocean had been conducted, such as Qinshan NPP in China (Nie *et al.*, 2020), France navy's nuclear-powered (Dufresne *et al.*, 2018), and Bushehr NPP in Iran (Hassanvand & Mirnejad, 2019). The ocean current was assumed to be the dominant factor in determining the distribution of radioactive ^{137}Cs in the waters, besides biological factors and chemical reactions (Kawamura *et al.*, 2017; Muslim *et al.*, 2017). In nuclear emergency, radioactive waste should not be disposed of immediately into the ocean. Instead, it was disposed of gradually in low volume to avoid the release of the large radioactive waste into the sea at one time (IAEA, 2009). This study simulated radioactive ^{137}Cs dynamics in several NPP waste volumes around West Kalimantan Sea. Furthermore,

these simulations can be considered to decide the best disposal system of those several waste volumes while nuclear emergency is occurred.

MATERIALS AND METHODS

This study simulated the water area from Mempawah Regency to Sambas Regency (Figure 1). The nuclear power plant was assumed to use the Pressurized Water Reactor (PWR) for reactor type, which was estimated to produce electrical energy around 330 MW (Nie *et al.*, 2020). International Atomic Energy Agency (2008) reported that the Pressurized Water Reactor produced about 250m³ of radioactive waste every year. Therefore, this study divided this annual radioactive waste volume into several disposal scenarios which were illustrated in Table 1. The activity limit of ^{137}Cs compound in NPP waste that is allowed to release in the sea is not larger than 5.10⁵ TBq during one year (Environment Agency, 2017). Base on annual data of waste volume and limited ^{137}Cs activity, this study assumed that the ^{137}Cs concentration in disposal radioactive waste was around 2.10⁵ Bq.m⁻³. The disposal waste discharge was assumed around 0.00278 m³s⁻¹, therefore the waste disposal duration of each scenario was approximately 1 hour (Scenario I), 5 hours (Scenario II), and 10 hours (Scenario III).

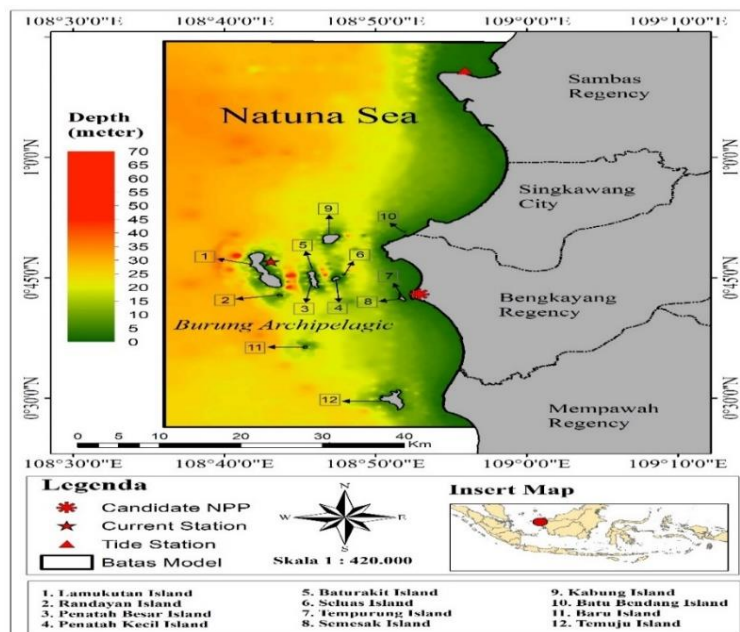


Figure 1. Boundary model and bathymetry

Table 1. Waste input scenario

Simulation	Waste Volume (m ³)	Disposal Duration	Waste Discharge (m ³ .s ⁻¹)	¹³⁷ Cs Concentration (Bq.m ⁻³)
Scenario I	10	1 hour		
Scenario II	50	5 hours	0,00278	2. 10 ⁵
Scenario III	100	10 hours		

The description of entire equation symbols were explained in Table 2. This study applied 2-dimensional numerical modeling to simulate the distribution of radioactive ¹³⁷Cs in the marine environment. This type of model was popularly applied in shallow water. By using 2-dimensional model, this study assumed : a) There was no vertical water current; b) water densities in each depth experienced the small change, then the depth average velocity was considered (Li *et al.*, 2021; Ouni *et al.*, 2020). The continuity equation (Equation 2) and momentum equations of x and y axis (Equation 3, 4) are fundamental formula to obtain temporally depth average velocities in each model grids, which are described respectively as (Deltares, 2014) :

$$\frac{\partial \zeta}{\partial t} + \frac{1}{\sqrt{G_x} \sqrt{G_y}} \frac{\partial((d+\zeta)U\sqrt{G_y}}{\partial x} + \frac{1}{\sqrt{G_x} \sqrt{G_y}} \frac{\partial((d+\zeta)V\sqrt{G_x}}{\partial y} = (d + \zeta)Q, \quad (1)$$

$$\frac{\partial u}{\partial t} + \frac{u}{\sqrt{G_x}} \frac{\partial u}{\partial x} + \frac{v}{\sqrt{G_y}} \frac{\partial u}{\partial y} + \frac{\omega}{d+\zeta} \frac{\partial u}{\partial z} - \frac{v^2}{\sqrt{G_x} \sqrt{G_y}} \frac{\partial \sqrt{G_y}}{\partial x} + \frac{uv}{\sqrt{G_x} \sqrt{G_y}} \frac{\partial \sqrt{G_x}}{\partial y} - f v = -\frac{1}{\rho_0 \sqrt{G_x}} P_x + F_x + \frac{1}{(d+\zeta)^2} \frac{\partial}{\partial z} \left(V_v \frac{\partial u}{\partial z} \right) + M_x \quad (2)$$

$$\frac{\partial v}{\partial t} + \frac{u}{\sqrt{G_x}} \frac{\partial v}{\partial x} + \frac{v}{\sqrt{G_y}} \frac{\partial v}{\partial y} + \frac{\omega}{d+\zeta} \frac{\partial v}{\partial z} + \frac{uv}{\sqrt{G_x} \sqrt{G_y}} \frac{\partial \sqrt{G_y}}{\partial x} + \frac{u^2}{\sqrt{G_x} \sqrt{G_y}} \frac{\partial \sqrt{G_x}}{\partial y} - f u = -\frac{1}{\rho_0 \sqrt{G_y}} P_y + F_y + \frac{1}{(d+\zeta)^2} \frac{\partial}{\partial z} \left(V_v \frac{\partial v}{\partial z} \right) + M_y \quad (3)$$

Furthermore, the ocean current considers to analyze the distribution of radioactive ¹³⁷Cs in coastal water through two processes, which are advection and diffusion. The advection process explains the radioactive dynamic base on the water current, while the diffusion process defines the dissolution of radioactive elements in the ocean (Kawamura *et al.*, 2017; Periañez *et al.*, 2019). In delft3d, the advection-diffusion formula is written as follows (Deltares, 2014):

$$\frac{\partial(d+\zeta)c}{\partial t} + \frac{1}{\sqrt{G_x} \sqrt{G_y}} \left\{ \frac{\partial[\sqrt{G_y}(d+\zeta)uc]}{\partial x} + \frac{\partial[\sqrt{G_x}(d+\zeta)vc]}{\partial y} \right\} + \frac{\partial \omega c}{\partial z} = \frac{d+\zeta}{\sqrt{G_x} \sqrt{G_y}} \left\{ \frac{\partial}{\partial x} \left[D_H \frac{\sqrt{G_y}}{\sqrt{G_x}} \frac{\partial c}{\partial x} \right] + \frac{\partial}{\partial y} \left[D_H \frac{\sqrt{G_x}}{\sqrt{G_y}} \frac{\partial c}{\partial y} \right] \right\} + \frac{1}{\partial+\zeta} \frac{\partial}{\partial z} \left(D_V \frac{\partial c}{\partial z} \right) - \lambda_d(d + \zeta)c + S \quad (4)$$

Finally, the simulated dispersion will provide distributional patterns and

concentrated changes of ¹³⁷Cs compound in the marine environment (Hassanvand & Mirnejad, 2019; Honda *et al.*, 2012; Kawamura *et al.*, 2017). This model results can be used to analyze their impact on aquatic ecosystems.

The stages of dispersed model development included collecting data; developing model grid; interpolating bathymetric data into the model grid; entering specified data into simulation program, and running the model. To start the simulation, we needed the specified data of 15-day tides, water bathymetry, coastline map, and surface winds. The simulation of ¹³⁷Cs dispersion had been constructed during 15 days through Delft3d-flow module to consider the neap tide and spring tide period in entire scenarios.

The ocean map derived by Hydrographic and Oceanographic Center of Indonesian Navy was processed through ArcGis 10.6 to obtain water bathymetries and shoreline data. Additionally, The National Bathymetry from Geospatial Information Agency (BIG) (<http://batnas.big.go.id/>) was also used to complete the bathymetry profile of near-coastal areas (Wisha *et al.*, 2018). There are many coordinate systems to define every positional point in the model boundary (Hassanvand & Mirnejad, 2019). This study chose the Universal Transverse Mercator (UTM) as the coordinate system in the simulation. The model grid was constructed through delft3d-grid in the resolution of about 100 m x 100 m ± 50 m. Furthermore, the bathymetry data processed by ArcGis 10.6 should be interpolated into entire grids to calculate their depths (Deltares, 2014).

Hourly 15-day tidal data was obtained by the tidal station of Geospatial Information Agency (<http://ina-sealevelmonitoring.big.go.id/ipasut/>) located in Pemangkat, Sambas Regency. The admiralty method was applied

in this study to derive astronomical components of ocean tide in the study location. Furthermore, those tidal astronomical components and time-series tide data were entered into the simulation program. Additionally, the tidal type of Gosong Coast could be determined by tidal astronomical components too through the formzhal formula (Irawan *et al.*, 2021).

This study derived x and y component data of surface wind from ERA 5 Satellite Marine Copernicus (<https://marine.copernicus.eu/>) with one-hour interval and 8 km resolution (Ssenyunzi *et al.*, 2020). We should convert those wind components into speed and direction of surface winds which were needed to run the simulation (Deltares, 2014).

The simulated results should be verified to decide whether the simulation has illustrated actual conditions. This study verified the model result of water current velocity and tide. Simulated tidal data was compared to time-series observed tide of Pemangkat BIG Station, while simulated water current velocity was verified by observed current velocity in the coastal area of Lamukutan Island which had been measured by previous research of Kushadiwijayanto & Apriansyah (2017). That previous research had measured hourly current velocity during 24 hours. The ¹³⁷Cs concentration was not verified because the nuclear reactor had not been built in Gosong Coast. Therefore, The model dispersion assumed that West Kalimantan Sea did not contain ¹³⁷Cs compound (Muslim *et al.*, 2016).

There were three popular equations to verify this simulation, such root mean square

error (RMSE), mean relative error (MRE), and coefficient of determination (R2), respectively expressed as follows (Hou *et al.*, 2020) :

$$RMSE = \sqrt{\frac{\sum_{i=1}^n (O_i - S_i)^2}{n}} \tag{5}$$

$$MRE = \frac{1}{n} \sum_{i=1}^n \frac{|S_i - M_i|}{M_i} \times 100 \% \tag{6}$$

$$R^2 = \frac{|\sum_{i=1}^{nd} (O_i - \bar{O})(S_i - \bar{S})|^2}{\sum_{i=1}^{nd} (O_i - \bar{O})^2 \sum_{i=1}^{nd} (S_i - \bar{S})^2} \tag{7}$$

The hydrodynamical model is accepted if the MRE value does not exceed 10% for tidal verification and 40% for current verification (Muslim *et al.*, 2016; Wisha *et al.*, 2018). Meanwhile, the better simulation is if the RMSE value is close to 0 and R2 is close to 1 (Hou *et al.*, 2020).

The model results of each scenario can consider to estimate the impact of NPP operation in Gosong Coast on marine organisms. Furthermore, the most efficient disposal waste scenario can be determined. This study analyzed it base on the calculation of the dose levels of various marine organisms on ¹³⁷Cs concentration which was obtained from entire scenario models by using Erica 1.3 tools (Giwa *et al.*, 2018; Steinhauser *et al.*, 2014). By specified data of ¹³⁷Cs concentration in the water column, The biota dose rate can be estimated through the concentration ratio of each organism group which is documented in erica data. Furthermore, we can calculate the biota dose rate of radioactive ¹³⁷Cs through these equations (Hosseini *et al.*, 2008):

$$Kd_i = \frac{C_i^{sed}}{C_i^{aq}} \tag{8}$$

$$CR_{j,i} = \frac{D_{j,i}}{C_i^{aq}} = \frac{D_{j,i}}{C_i^{sed}} \tag{9}$$

Table 2. Formula symbol description

u, v, ω	Water velocity	f_v, f_u	Coriolis force
G_x, G_y	Transformed coordinate coefficient	V_v	Vertical eddy viscosity
d	Depth	F_x, F_y	Tubulent motion flow
ζ	Water level	O	Observed data
c	¹³⁷ Cs concentration	S	Simulated data
D_H, D_v	Diffusion coefficient	n	Total of data
λ_d	Decay rate	Kd	Distribution coefficient
ρ_0	Water density	C^{sed}	Concentration in sediment
S	Discharge	C^{aq}	Concentration in water column
P_x, P_y	Hydrostatic pressure	CR	Concentration ratio
M_x, M_y	Momentum coefficient	D	Dose rate

RESULT AND DISCUSSION

The coastal water of Gosong Coast have mixed semidiurnal tidal types (Formzhal = 1.06). It means that this coastal area sometimes experiences twice flood tide and twice ebb tides with different tidal co-range and tidal co-phase. Gosong coast is quite shallow water with its depth range below 5 m (Figure 1). The shallow water topography increased friction force between water masses and bottom sediment, thus this coastal water generally had the lower current velocity (Akbar *et al.*, 2017).

The comparison graphs between observed data and simulated data were presented in Figure 2. After the model verification, tidal and current velocity model error values were respectively 7.58% and 39.63% for MRE; 0.08 and 0.1 for RMSE; 92% and 70% for R². These error values were comparable to previous studies (Table 3). This model did not consider entire parameters which influenced the hydrodynamical condition in the marine environment, such as rainfall, water density gradients, and coastal community activities (Mejia-Olivares *et al.*, 2020). Additionally, the grid resolution and interval of model configuration may influence the model result too (Hou *et al.*, 2020). Therefore, it is almost impossible for ocean dynamic simulation to perfectly illustrate the actual condition. However, the simulation errors in this study were still tolerated. Thus, this hydrodynamical model can be considered to define several scenarios of radioactive waste distribution.

Figure 3 illustrated ocean current patterns of Northern West Kalimantan Sea in

each tidal condition. The ocean current directions did not show significant differences among spring and neap tide periods, however current velocities during spring period dominantly increased rather than current velocities in the neap period. The amount of current velocities on coastal water ranged from 0.01 – 0.3 m.s⁻¹, thus current velocities increased towards offshore. The water flow in Gosong Coast showed the different pattern among flood and ebb tide. During ebb tide, ocean currents at Gosong Beach moved directly towards offshore through the water area of Burung Archipelagic. Meanwhile, ocean currents in Gosong Coast flowed towards the coastal area of Singkawang City before they deflected towards offshore during high tide. However, not entire ocean currents in Singkawang Coastal Water deflected to offshore, but there were a few of those water currents which flowed to Sambas Sea. In general, the ocean current of the Northern West Kalimantan Sea relatively flowed parallel to the coastline. This phenom was popular which occurred in various open seas (Mayerle *et al.*, 2020). In contrast, ocean currents dominantly moved towards the coastline at flood tide and move away from the coastal area at ebb tide in the enclosed sea, such as estuary or bay (Hendrawan & Asai, 2014; Wisha *et al.*, 2018).

Figure 4 illustrates temporally radioactive ¹³⁷Cs dynamics of each scenario in West Kalimantan Sea along with its decreased concentration. After 24 hours of radioactive waste disposal, ¹³⁷Cs liquid was estimated to have spread to Burung Archipelagic Sea. Scenario 1 showed decrease rates of ¹³⁷Cs concentration below 52 Bq.m⁻³, while the concentration is still above 100 Bq.m⁻³ for

Table 3. Comparison of Error Values Among Various Researches

Parameter	MRE (%)	RMSE	R ² (%)	Reference
Water Level	7.58	0.08	92	This Research
	0.8-1.53	0.028-0.067	88-99	(Hou <i>et al.</i> , 2020)
	31.99	-	-	(Muslim <i>et al.</i> , 2016)
	-	0.09	-	(Wisha <i>et al.</i> , 2018)
	-	0.82	-	(Akpinar <i>et al.</i> , 2012)
Ocean Velocity	39.63	0.1	70	This Research
	-	0.01 – 0.57	-	(Mejia-Olivares <i>et al.</i> , 2020)
	-	0.03 – 1.46	-	(Chatzirodou <i>et al.</i> , 2017)
	-	0.1-0.12	-	(Wisha <i>et al.</i> , 2018)

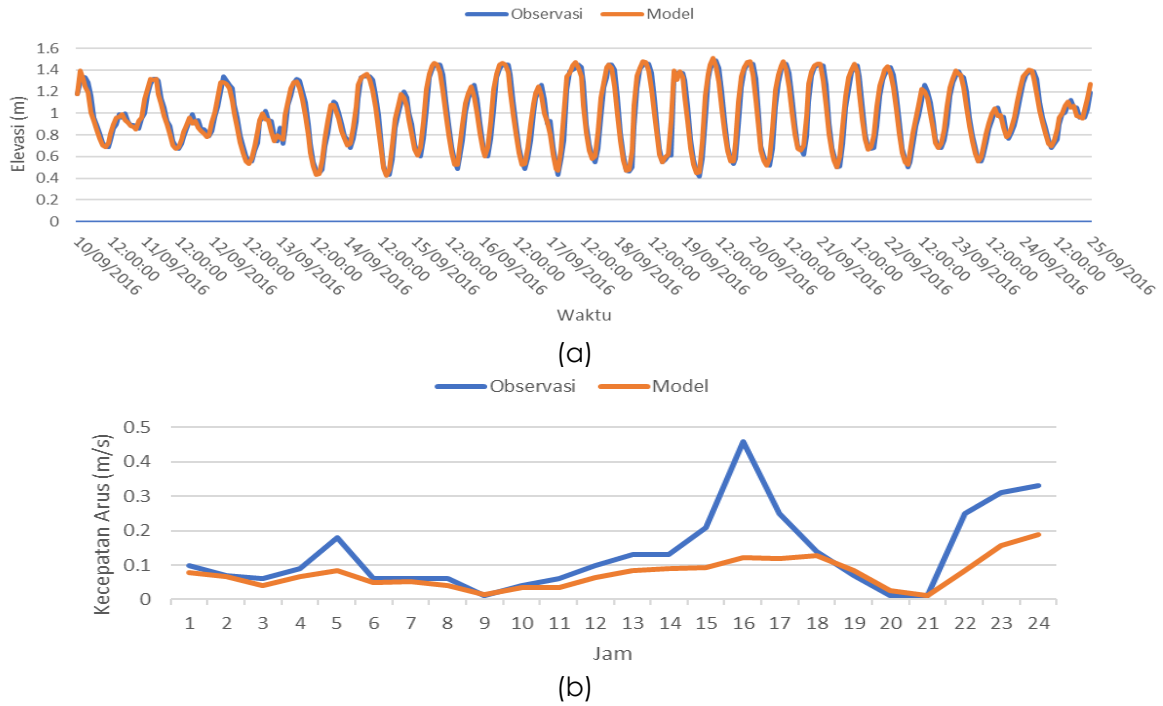


Figure 2. Validation data; (a) water elevation, (b) depth average velocity

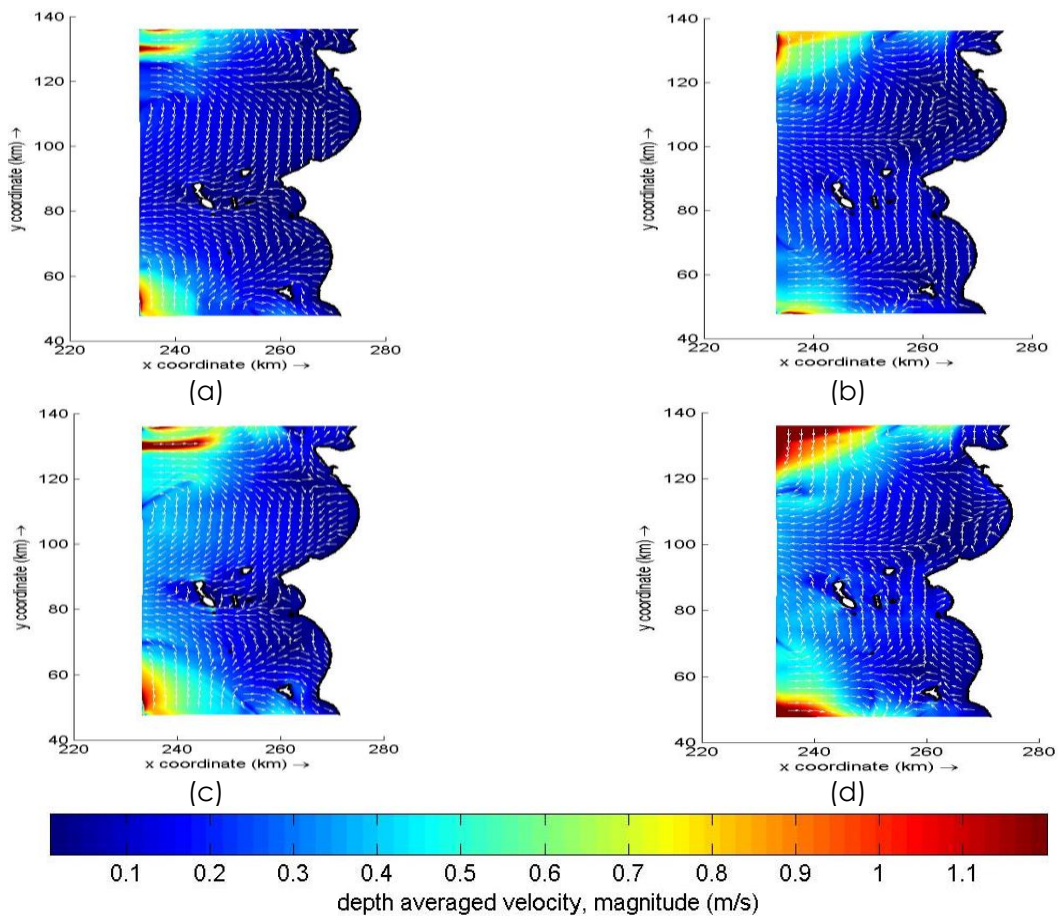


Figure 3. Ocean current, (a) flood neap tide, (b) ebb neap tide, (c) the highest flood spring tide, (d) the lowest ebb spring tide

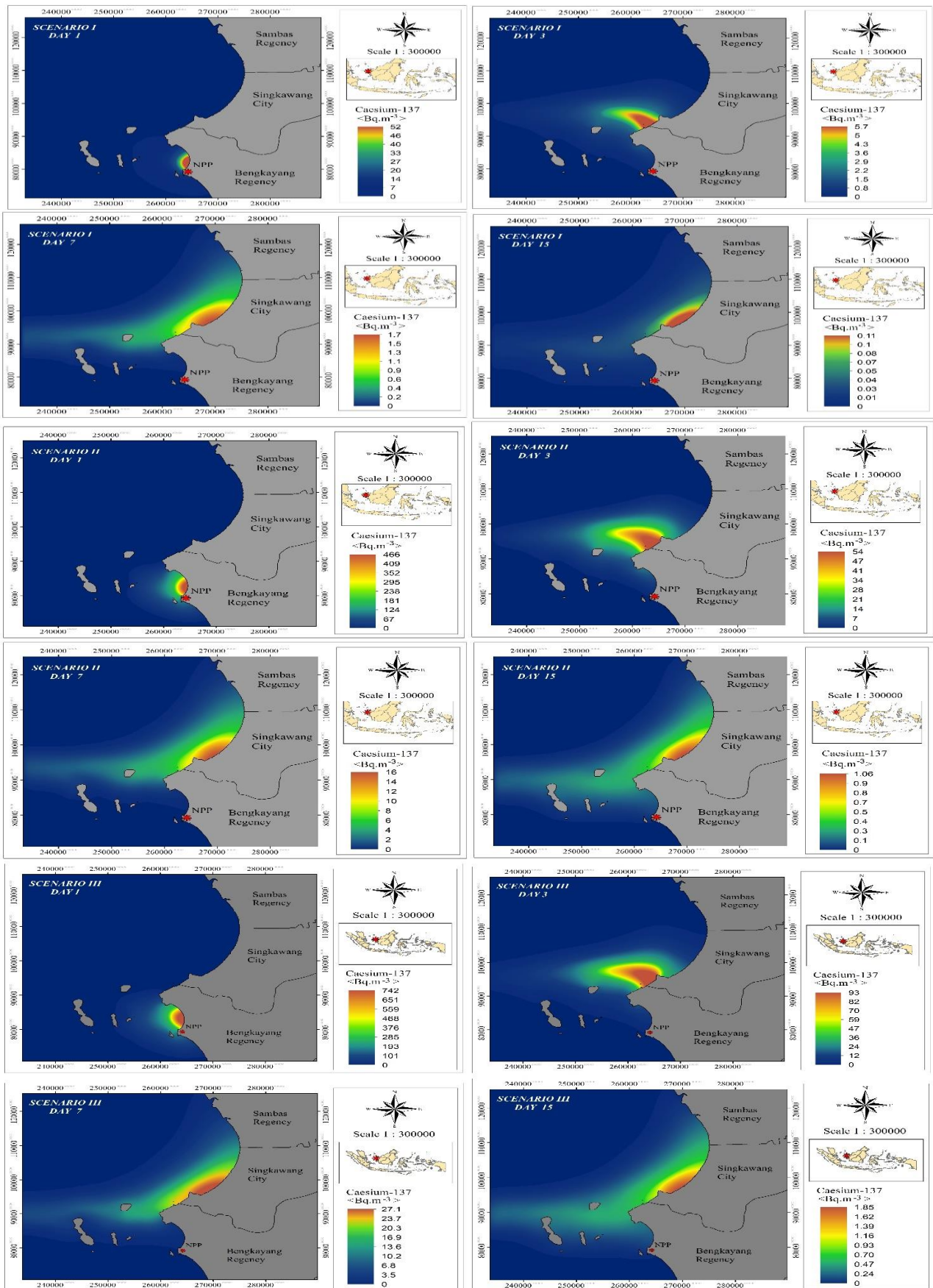


Figure 4. ^{137}Cs disperse simulation

Scenarios II and III. Scenario III showed that the expansion of ¹³⁷Cs substrate had reached the eastern coast of Penata Besar Island, while Scenario I and II were predicted to still reach Penata Kecil Island. Nevertheless, radioactive ¹³⁷Cs reached the Bird Archipelagic Sea with lower concentrations instead of the northern coastal water of Gosong Coast. The dissolved ¹³⁷Cs was accumulated on the large scale in the northern coastal waters of Gosong Coast after the first day of its dispersions.

The 3rd day of the simulation was marked by the spreading of ¹³⁷Cs radioactive to the coastal sea of Singkawang City. Each scenario did not illustrate the different pattern on ¹³⁷Cs dispersion. ¹³⁷Cs concentrations in Scenario I experienced rapid declines rather than other scenarios. The concentrations of ¹³⁷Cs dissolve were below 5.8 Bq.m⁻³ in Scenario I, while Scenario II and III ranged their maximum concentration about 54 Bq.m⁻³ and 93 Bq.m⁻³ respectively. The Bengkayang Sea has shown the sharp decrease of ¹³⁷Cs activity after 3rd day of discharge.

The dissolved ¹³⁷Cs continued to spread toward the Sambas Coastal Sea after 3rd day of discharge. This radionuclide liquid was marked to reach the large area of Sambas Coastal Sea on the 7th day of simulation. However, The Sambas Coastal Sea derived the dissolved ¹³⁷Cs with quite low concentrations, therefore it will minimize the chance of water pollution in that sea due to radioactive waste dumping at Gosong Coast. ¹³⁷Cs

concentrations were accumulated at higher scale in Singkawang Coastal Sea.

Dissolved ¹³⁷Cs spread steadily to offshore after the seventh day of radioactive waste disposal. it meant that the concentration of dissolved ¹³⁷Cs in coastal waters will continue to decrease due to the distribution of dissolved ¹³⁷Cs to offshore. During the 15 days of simulation, the maximum concentrations in Scenarios I, II, and III reached respectively about 0.11 Bq.m⁻³, 1.06 Bq.m⁻³, and 1.85 Bq.m⁻³. The Singkawang Coastal Sea still showed the highest ¹³⁷Cs activity range rather than other water areas on 15th day of discharge.

Furthermore, this study calculated the dose rate of dissolved ¹³⁷Cs on several marine organisms to estimate the environmental impact of various ¹³⁷Cs concentrations contained in this sea. This Study only involved the maximum value of each scenario on 1st day of simulation to obtain the dose rate on marine organisms. Table 4 presents some ¹³⁷Cs dose rates in 12 groups of marine organisms by using Erica Tools. Base on the dose rate analysis, all dose rates on each organism group showed the figure below their dose limits in entire scenarios. It meant that the ¹³⁷Cs activity from radioactive waste after 1st day of discharge had decreased into the value range which was tolerated by marine organism. This study assumed that the each ¹³⁷Cs disposal scenario will not give any pollution impacts in the large scale of marine environment.

Table 4. Total dose rate day – 1 on various scenarios and general dose limit

Biota	Total Dose Rate			Dose Limit		
	Scenario I	Scenario II	Scenario III	Morbidity	Mutation	Mortality
Benthic Fish	8.45.10 ⁻²	7.52.10 ⁻¹	1.20	1.38	3.58	12.5
Crustacean	8.15.10 ⁻²	7.25.10 ⁻¹	1.15	0.58	-	-
Macroalgae	9.27.10 ⁻²	8.25.10 ⁻¹	1.31	2.41	-	-
Mammal	3.81.10 ⁻³	3.39.10 ⁻²	5.40.10 ⁻²	10	-	-
Mollusc - bivalve	8.97.10 ⁻²	7.99.10 ⁻¹	1.27	16.7	-	1000
Pelagic Fish	8.07.10 ⁻⁴	7.19.10 ⁻³	1.14.10 ⁻²	1.38	3.58	12.5
Phytoplankton	5.10.10 ⁻⁵	4.54.10 ⁻⁴	7.22.10 ⁻⁴	2.41	-	-
Polychaete	1.86.10 ⁻¹	1.65	2.63	0.83	14	-
Reptile	8.05.10 ⁻³	7.17.10 ⁻²	1.14.10 ⁻¹	-	-	-
Anemones and Coral	9.38.10 ⁻²	8.35.10 ⁻¹	1.33	-	-	-
Vascular plant	8.94.10 ⁻²	7.96.10 ⁻¹	1.27	2.41	-	-
Zooplankton	8.36.10 ⁻⁴	7.44.10 ⁻³	1.18.10 ⁻²	1.54	-	-

(Refrence : Erica Tool Software)

If this study result was compared to previous research, the concentration dilution rate in West Kalimantan Sea was relatively slower than in Hangzhou Bay. Figure 4 illustrated that ^{137}Cs concentrations decreased about 10^4 Bq.m^{-3} after the 7th day of discharge, while the decreased rate of tritium concentration from Quinshan Nuclear Power Plant (China) with the same reactor type had reached around $10^{10} \text{ Bq.m}^{-3}$ after the 4th day of discharge (Nie *et al.*, 2020). Gosong coastal sea is shallow water with low flow velocities. Ocean current plays the balance role of each pollutant in the marine environment, while it spread these pollutants towards the wide area and decreases their concentrations (Hassanvand & Mirnejad, 2019). In addition, shallow water increases the chance of accumulation of radioactive ^{137}Cs in bottom sediments (Dufresne *et al.*, 2018). Therefore, it should be considered about the amounts of liquid radionuclide which will be discharged into Gosong Coastal Sea. Nevertheless, this study concluded that there were no significant differences in environmental impacts at each scenario.

CONCLUSION

The distribution of radioactive ^{137}Cs from Gosong Coast for 15 days was estimated to reach the coastal areas of Burung Archipelagic, Singkawang City, and Sambas Regency. This study concluded that each scenario of disposal systems did not experience any pollution impacts in the marine environment after 1st day of discharge. This statement referred to dose rate values of each aquatic organism which showed figures below the dose limit at entire scenarios. Furthermore, each scenario can be applied to discharge the ^{137}Cs radioactive waste if the nuclear emergency is occurred during NPP's operation.

ACKNOWLEDGEMENT

This research was the result of the collaboration between National Nuclear Energy Agency and Diponegoro University. Authors would like to thank to Center for Radiation Safety and Metrology of BATAN that had provided opportunities for several students of Diponegoro University to collaborate on research.

REFERENCES

- Akbar, A.A., Sartohadi, J., Djohan, T.S., & Ritohardoyo, S. 2017. The Role of Breakwaters on The Rehabilitation of Coastal and Mangrove Forests in West Kalimantan, Indonesia. *Ocean and Coastal Management*, 138:50–59. doi : 10.1016/j.ocecoaman.2017.01.004
- Akpinar, A., van Vledder, G.P., Kömürçü, M.I., & Özger, M. 2012. Evaluation of the numerical wave model (SWAN) for wave simulation in the Black Sea. *Continental Shelf Research*, 50:80–99. doi : 10.1016/j.csr.2012.09.012
- Alkatiri, A., Suseno, H., Hudiyono, S., & Moersidik, S.S. 2019. The Distribution of Radiocesium in The Indian Ocean and Its Relation To The Exit Passage of The Indonesian Throughflow. *Regional Studies in Marine Science*, 25:1-8. doi : 10.1016/j.rjsma.2018.100496
- Aoyama, M., Tsumune, D., Inomata, Y., & Tateda, Y. 2020. Mass Balance and Latest Fluxes of Radiocesium Derived from The Fukushima Accident in The Western North Pacific Ocean and Coastal Regions of Japan. *Journal of Environmental Radioactivity*, 217:106206. doi : 10.1016/j.jenvrad.2020.106206
- Chatzirodou, A., Karunarathna, H., & Reeve, D. E. 2017. Modelling 3D Hydrodynamics Governing Island-Associated Sandbanks in a Proposed Tidal Stream Energy Site. *Applied Ocean Research*, 66:79–94. doi : 10.1016/j.apor.2017.04.008
- Deltares. 2014. *3D/2D Modelling Suite for Integral Water Solutions: Hydro-Morphodynamics*. 710.
- Dufresne, C., Duffa, C., Rey, V. & Verney, R. 2018. Hydro-sedimentary Model as a Post-Accidental Management Tool: Application To Radionuclide Marine Dispersion in The Bay of Toulon (France). *Ocean and Coastal Management*, 153: 176–192. doi : 10.1016/j.ocecoaman.2017.12.026
- Environment Agency. 2017. Generic Design Assessment AP1000 Nuclear Power Plant Design By Westinghouse Electric Company LCC.
- Fulghum, C.M., DiBona, E.R., Leaphart, J.C., Korotasz, A.M., Beasley, J.C., & Bryan, A.L. 2019. Radiocesium (^{137}Cs) Accumulation

- By Fish Within a Legacy Reactor Cooling Canal System on The Savannah River Site. *Environment International*, 126:216–221. doi : 10.1016/j.envint. 2019.02.039
- Giwa, K.W., Osahon, O.D., Amodu, F.R., Tahiru, T.I. & Ogunsanwo, F.O. 2018. Radiometric Analysis and Spatial Distribution of Radionuclides with-In The Terrestrial Environment of South-Western Nigeria Using ERICA Tool. *Environmental Nanotechnology, Monitoring and Management*, 10:419–426. doi : 10.1016/j.enmm.2018.10.002
- Hassanvand, M., & Mirnejad, Z. 2019. Progress in Nuclear Energy Hydrodynamic Model of Radionuclide Dispersion During Normal Operation and Accident of Bushehr Nuclear Power Plant. *Progress in Nuclear Energy*, 116:115–123. doi : 10.1016/j.pnuene.2019.04.002
- Hendrawan, I. G., & Asai, K. 2014. Numerical Study on Tidal Currents and Seawater Exchange in The Benoa Bay, Bali, Indonesia. *Acta Oceanologica Sinica*, 33(3):90–100. doi : 10.1007/s13131-014-0434-5
- Honda, M.C., Aono, T., Aoyama, M., Hamajima, Y., Kawakami, H., Kitamura, M., Masumoto, Y., Miyazawa, Y., Takigawa, M. & Saino, T. 2012. Dispersion of Artificial Caesium-134 and -137 in the Western North Pacific One Month After The Fukushima Accident. *Journal Geochem*, 46(1):e1–e9.
- Hosseini, A., Thørring, H., Brown, J. E., Saxén, R., & Illus, E. 2008. Transfer of Radionuclides in Aquatic Ecosystems - Default Concentration Ratios for Aquatic Biota in the Erica Tool. *Journal of Environmental Radioactivity*, 99(9):1408–1429. doi : 10.1016/j.jenvrad.2008.01.012
- Hou, J., Kang, Y., Hu, C., Tong, Y., Pan, B., & Xia, J. 2020. A Gpu-Based Numerical Model Coupling Hydrodynamical and Morphological Processes. *International Journal of Sediment Research*, 35(4), 386–394. doi : 10.1016/j.ijsrc.2020. 02.005
- IAEA. 2008. Estimation of Global Inventories of Radioactive Waste and Other Radioactive Materials (Issue June).
- IAEA. 2009. Policies and Strategies for Radioactive Waste. *International Atomic Energy Agency, No. NW-G-1*, 1–57.
- Irawan, A.M., Marfai, M.A., Munawar, Nugraheni, I.R., Gustono, S.T., Rejeki, H.A., Widodo, A., Mahmudiah, R.R., & Faridatunnisa, M. 2021. Comparison Between Averaged and Localised Subsidence Measurements for Coastal Floods Projection in 2050 Semarang, Indonesia. *Urban Climate*, 35(May 2020), 100760. doi : 10.1016/j.uclim. 2020.100760
- Kawamura, H., Furuno, A., Kobayashi, T., In, T., Nakayama, T., Ishikawa, Y., Miyazawa, Y., & Usui, N. 2017. Oceanic Dispersion of Fukushima-Derived Cs-137 Simulated By Multiple Oceanic General Circulation Models. *Journal of Environmental Radioactivity*, 180:36–58. doi : 10.1016/j.jenvrad.2017.09.020
- Kushadiwijayanto, A.A., & Apriansyah. 2017. Pemodelan Arus Musiman di Perairan Lemukutan Kalimantan. *Porseding Semirata 2017 Bidang MIPA BKS-PTN Wilayah Barat, January 2018*.
- Li, L., Cheng, R., & Ge, H. 2021. New Feedback Control for a Novel Two-Dimensional Lattice Hydrodynamic Model Considering Driver's Memory Effect. *Physica A: Statistical Mechanics and Its Applications*, 561:125295. doi : 10.1016/j.physa.2020.125295
- Mayerle, R., Niederndorfer, K.R., Fernández Jaramillo, J.M., & Runte, K.H. 2020. Hydrodynamic Method for Estimating Production Carrying Capacity of Coastal Finfish Cage Aquaculture in Southeast Asia. *Aquacultural Engineering*, 88:102038. doi : 10.1016/j.aquaeng.2019. 102038
- Mejia-Olivares, C. J., Haigh, I. D., Lewis, M. J., & Neill, S.P. 2020. Sensitivity Assessment of Bathymetry and Choice of Tidal Constituents on Tidal-Stream Energy Resource Characterisation in The Gulf of California, Mexico. *Applied Ocean Research*, 102:102281. doi : 10.1016/j.apor.2020.102281
- Muslim, M., Suseno, H., & Saodah, S. 2016. Condition of ¹³⁷Cs Activity in Karimunjawa Waters and Its Distribution When an NPP Jepara is Operated. *Ilmu Kelautan: Indonesian Journal of Marine Sciences*, 21(3):143-150. doi : 10.14710/ik.ijms.21.3. 143-150
- Muslim, M., Suseno, H., & Pratiwi, M.J. 2017. Behavior of ¹³⁷Cs Activity in the Sayung Waters, Demak, Indonesia. *Atom*

- Indonesia. 43(1):41-46. doi : 10.17146/aij.2017.588
- Nie, B., Yang, J., Wang, W., Gu, Z., Yuan, Y., & Li, F. 2020. Numerical Study on Tritium Dispersion in Coastal Waters : The Case of Hangzhou Bay, China. *Journal of Hydrology*, 590: 125532. doi : 10.1016/j.jhydrol.2020.125532
- Ouni, H., Sousa, M.C., Ribeiro, A.S., Pinheiro, J., Ben M'Barek, N., Tarhouni, J., Tlatli-Hariga, N., & Dias, J.M. 2020. Numerical Modeling of Hydrodynamic Circulation in Ichkeul Lake-Tunisia. *Energy Reports*, 6:208–213. doi : 10.1016/j.egy.2019.08.044
- Pemprov Kalimantan Barat. 2019. Rencana Umum Energi Daerah. <https://esdm.kalbarprov.go.id/wp-content/uploads/2020/07/Draft-Narasi-RUED-P-Kalbar.pdf>
- Periáñez, R, Bezhenar, R., Brovchenko, I., Duffa, C., Iosjpe, M., Jung, K.T., & Kim, K.O. 2019. *Marine Radionuclide Transport Modelling: Recent Developments, Problems and Challenges*. 122 (July 2018).
- Periáñez, Raúl, Qiao, F., Zhao, C., de With, G., Jung, K. T., Sangmanee, C., Wang, G., Xia, C., & Zhang, M. 2021. Opening Fukushima floodgates: Modelling ¹³⁷Cs Impact in Marine Biota. *Marine Pollution Bulletin*, 170: p.112645. doi: 10.1016/j.marpolbul.2021.112645
- Presidential Decree. 2006. The National Energy Policy. *Peraturan Pemerintah Republik Indonesia Nomor 26 Tahun 1985 Tentang Jalan* (Issue 1). <https://www.google.com/url?sa=t&rct=j&q=&esrc=s&source=web&cd=1&cad=rja&uact=8&ved=2ahUKEwjWxrKeif7eAhVYfysKHcHWAOWQFjAAegQICRAC&url=https%3A%2F%2Fwww.ojk.go.id%2Fid%2Fkanal%2Fpasar-modal%2Fregulasi%2Fundang-undang%2FDocument>
- s%2FPages%2Fundang-undang-nomo
- Sakuma, K., Nakanishi, T., Yoshimura, K., Kurikami, H., Nanba, K., & Zheleznyak, M. 2019. A Modeling Approach To Estimate The ¹³⁷Cs Discharge in Rivers from Immediately after The Fukushima Accident until 2017. *Journal of Environmental Radioactivity*, 208–209:106041. doi : 10.1016/j.jenvrad.2019.106041
- Ssenyunzi, R.C., Oruru, B., D'ujanga, F.M., Realini, E., Barindelli, S., Tagliaferro, G., von Engeln, A., & van de Giesen, N. 2020. Performance of ERA5 Data in Retrieving Precipitable Water Vapour Over East African Tropical Region. *Advances in Space Research*, 65(8):1877–1893. doi : 10.1016/j.asr.2020.02.003
- Steinhauser, G., Brandl, A., & Johnson, T.E. 2014. Comparison of The Chernobyl and Fukushima Nuclear Accidents: A Review of The Environmental Impacts. *Science of the Total Environment*, 470:800–817. doi : 10.1016/j.scitotenv.2013.10.029
- Tsumune, D., Tsubono, T., Misumi, K., Tateda, Y., Toyoda, Y., Onda, Y., & Aoyama, M. 2020. Impacts of Direct Release and River Discharge on Oceanic ¹³⁷Cs Derived from The Fukushima Dai-ichi Nuclear Power Plant Accident. *Journal of Environmental Radioactivity*, 214:p106173. doi : 10.1016/j.jenvrad.2020.106173
- Wisha, U.J., Tanto, T. Al, Pranowo, W.S., & Husrin, S. 2018. Current Movement in Benoa Bay water, Bali, Indonesia: Pattern of Tidal Current Changes Simulated for The Condition before, during, and after Reclamation. *Regional Studies in Marine Science*, 18:177–187. doi : 10.1016/j.rsma.2017.10.006